EFFECTS OF THE INTRINSIC THREE-DIMENSIONALIZATION OF LAMINAR SEPARATION BUBBLES ON THE AMPLIFICATION OF EXTERNAL DISTURBANCES

Daniel Rodríguez* , **Elmer M. Gennaro****

Laboratory of Theoretical and Applied Mechanics (LMTA), Graduate Program in Mechanical Engineering (PGMEC), Department of Mechanical Engineering, Universidade Federal Fluminense, Brazil , * São Paulo State University (UNESP), Campus São João da Boa Vista, Brazil**

Keywords: *Flow separation; Laminar-turbulent transition; Flow instability; Laminar separation bubble*

Abstract

The size and behavior of laminar separation bubbles is strongly related to the laminar-to-turbulent transition process that takes place downstream of the separation of the laminar boundary layer. Wind-tunnel experiments and numerical simulations in which external fluctuations are imposed show a clear dominance of instability waves of convective nature in the transition process. On the other hand, stability analysis demonstrate the existence of a self-excited mechanism that introduces a three-dimensionalization of the recirculation region. This paper studies the co-existence of both mechanisms, i.e. how the spanwise modulation of the bubbles can alter the properties of instability waves. It is found that a large convective amplification is induced by the spanwise velocity gradients.

1 Introduction

Separation bubbles have the potential to amplify external disturbances in a explosive manner: the orders-of-magnitude amplitude growth resulting from convective instability mechanisms typically leads to strong non-linear phenomena and transition to turbulence, even at low excitation levels [5, 1, 4, 8]. Some researchers investigated the origin of three-dimensionality under these circumstances, attributing it mainly to secondary instabilities of the spanwise vortices shed from the bubble [11, 8]. Rist and Maucher [10] investigated the non-linear interactions occurring when two oblique waves were excited, finding that the transition occurred in an abrupt manner (which they termed *oblique breakdown*) more similar to the experimental observations, than under other forcing conditions in which the dominant component was 2D.

The absence of external excitation neglects the amplifier behavior of the bubbles, and only self-excited global instabilities have the potential of initiating the transition process. Recently[14] it was demonstrated that the 3D global instability mode existing in LSBs [20, 16] becomes active for LSBs that are significantly weaker (with a reversed-flow magnitude $u_{rev} \sim 7-8\%$) than required for the onset of self-sustained two-dimensional oscillations ($u_{rev} \sim 16-20\%$) [1, 11]. On the other hand, the presence of spanwise gradients in the 3D base flow as well as spanwise sections with a peak recirculation u_{rev} higher than that of the baseline 2D LSB suggests that the primary centrifugal instability can enhance the amplifier character of the separation bubbles. In this respect, it is worth noting that experimental and numerical studies observed the spontaneous appearance of streamwise streaks [21, 19] or three-dimensionality [4] underlying the dominant convective instability and without explic-

itly imposing them. An extension of the Parabolized Stability Equations (PSE) that considers three-dimensional (with one slowly-diverging direction) base flows, sometimes referred to as 3D-PSE [6, 3], is employed in this respect.

2 3D separation bubbles resulting from self-excited instability

2.1 Baseline separation bubbles

Baseline LSBs are computed using an inverse nonsimilar boundary-layer formulation in which a streamwise distribution of the displacement thickness is prescribed. For a bounded streamwise extent, the displacement thickness is smoothly increased over the corresponding value for a zero-pressure-gradient boundary layer. The streamwise extent of the displacement thickness increase is fixed, and different decelerated flows are computed by varying the peak displacement thickness $\bar{\delta}_{max}$. Fully laminar, two-dimensional and steady flows with a closed recirculation region are computed in this manner.

2.2 Self-excited linear global instability

Global eigenmode analyses, considering modal perturbations of the form $\hat{\mathbf{q}}(x,y)\exp[\mathrm{i}(\beta z-\omega t)]$, show that the three-dimensional centrifugal instability is the only self-excited linear mechanism active in the present baseline LSBs. This instability is characterized by: (i) its frequency $\omega = 0$; (ii) it is not active for two-dimensional perturbations; (iii) it has a preferential wavenumber $\beta_c \approx 0.166$ for the present LSBs; and (iv) it becomes active for reversed flow larger than $u_{0,rev} \approx 6.98\%$. Detailed information on the primary instability analyses can be found elsewhere [14].

2.3 Non-linear evolution and growth saturation

Direct numerical simulations are carried out to study the subsequent non-linear evolution of the flow. A supercritical pitchfork bifurcation is recovered, as shown in figures 1 and 2. The interactions between the fundamental wavenumber of the primary instability with its harmonics and the distortion of the spanwise-average component lead to disturbance growth saturation. The three-dimensional flows at saturated conditions are denoted by $\mathbf{q}_{3D}$ in what follows, while $\mathbf{q}_{2D}$ refers to their spanwise average. While the centrifugal instability reduces the mean bubble recirculation, the spanwise modulation of the separated shear layer results in localized peak reversed flow greater than $u_{3D,rev} = 10\%$.

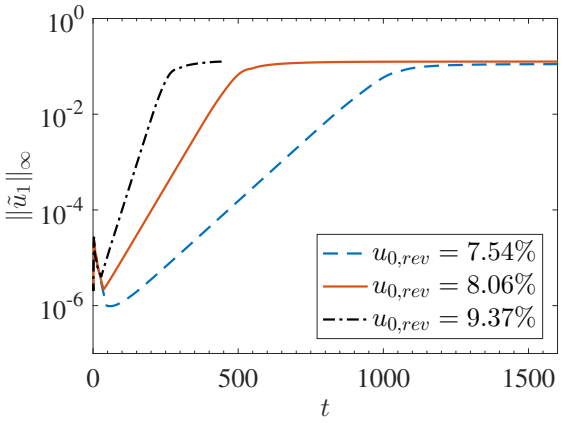

Fig. 1 Temporal evolution of the fundamental spanwise mode, quantified by $\|\tilde{u}_1\|_\infty$, for different baseline LSBs.

Figure 3(a) shows the baseline LSB together with the streamwise velocity components of the linear eigenmode corresponding to the primary instability, while figure 3(a) shows the corresponding distorted separation bubble after non-linear saturation, $\bar{u}_{3D}$. Colour contours illustrate the strong modification of the disturbance component on account of non-linearities, as well as the formation of a streamwise streak downstream of the peak deceleration within the LSB.

3 Convective amplification of disturbance waves

3.1 3D Parabolized Stability Equations

Linear amplification of incoming disturbance waves is studied using Parabolized Stability Equations (PSE). The classic PSE approach is extended here to three-dimensional base flows

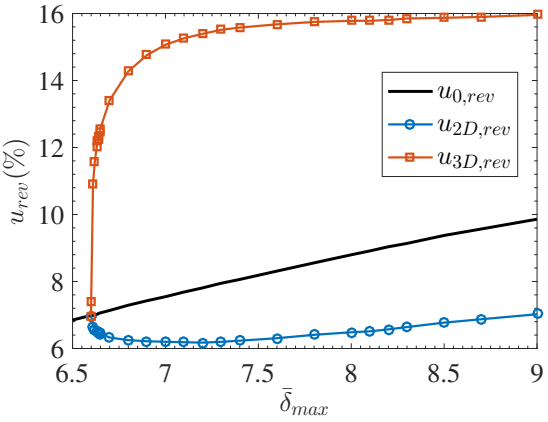

Fig. 2 Bifurcation diagram of the primary instability, corresponding to the saturation of the three-dimensional instability. Peak reversed flow of the baseline LSB ($u_{0,rev}$); the saturated three-dimensional flow ($u_{3D,rev}$), and the spanwise-averaged saturated flow ($u_{2D,rev}$)

that depend strongly on two spatial directions and only mildly on the streamwise one: disturbances of the form

$$\mathbf{q}'(x,y,z,t) = \hat{\mathbf{q}}(X,y,z)\exp\left[\mathrm{i}\left(\int_{x'}\alpha(X')dx' - \omega t\right)\right] + c.c. \quad (1)$$

are considered, where $\hat{\mathbf{q}}(X,y,z)$ is the shape function and $\alpha(X')$ is a streamwise wavenumber which depends on the slow variable X. Introduction of this decomposition into the Navier Stokes equations in disturbance form, one obtains the matrix problem

$$\mathcal{R}\frac{\partial\hat{\mathbf{q}}}{\partial X} = \mathcal{L}\hat{\mathbf{q}} + \mathbf{F}(\hat{\mathbf{q}},\hat{\mathbf{q}}). \quad (2)$$

PSE can take into account non-linear interactions between the different frequency Fourier modes, through the coupling term $\mathbf{F}$. The marching algorithm in PSE requires of a normalization condition to isolate the slow variations of the shape function $\hat{\mathbf{q}}$ from the fast-scale oscillations and spatial growth. Here, the following normalization condition [6] is used

$$\int_y\int_z \hat{\mathbf{q}}^*\frac{\partial\hat{\mathbf{q}}}{\partial X}\,dydz, \quad (3)$$

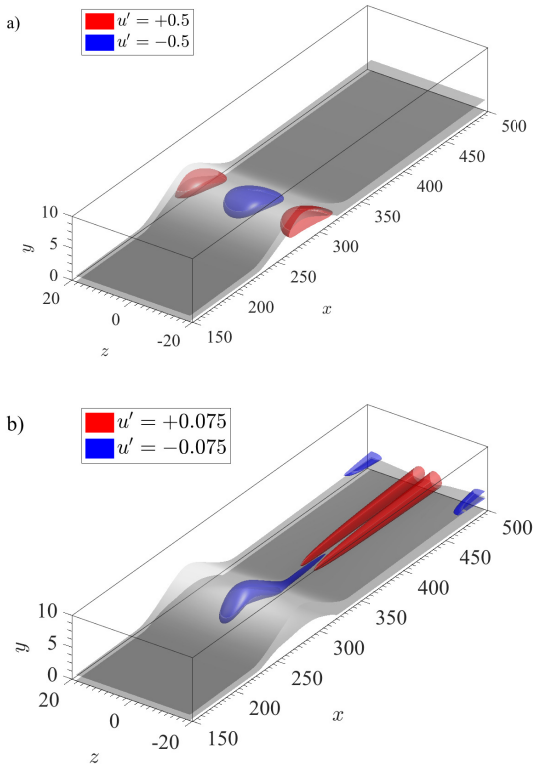

Fig. 3 (a) Baseline LSB and eigenmode corresponding to the primary instability. Nearly-horizontal grey surfaces correspond to $u_0 = 0$ and 0.5. The surfaces correspond to $u' = \pm 0.5\|u'\|_\infty$ of the eigenfunction's streamwise velocity component. (b) Steady three-dimensional LSB resulting from the saturation of the primary instability. The horizontal grey surface corresponds to $\bar{u}_{3D} = 0$ and 0.5. Disturbance streamwise velocity component u'. Baseline LSB with $\bar{\delta}_{max} = 7.4$, $u_{0,rev} = 8.06\%$

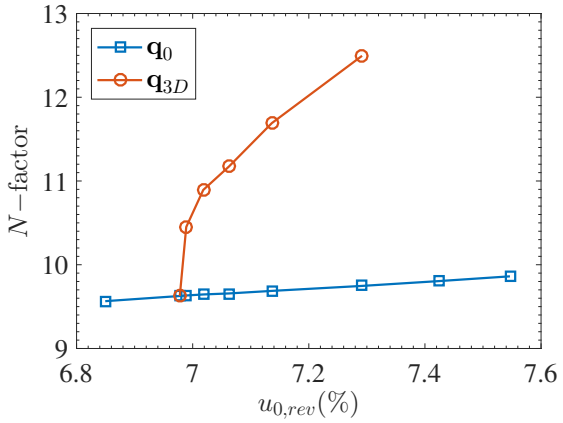

Fig. 4 Maximum $N-$factor for baseline LSBs $\mathbf{q}_0$ and three-dimensional LSBs $\mathbf{q}_{3D}$, as a function of $u_{0,rev}$.

which provides an condition for the iterative calculation of α. The superscript $*$ denotes complex conjugation. This approach, being an straightforward extension of the classic PSE, was not successfully implemented until [3] due to its computational cost.

Numerical solution of both the PSE requires the spatial discretization of the two-dimensional linear operators **R** and **L** in the cross-stream (y,z) planes. A new stability code was used [12], that combines variable-stencil high-order finite differences and sparse algebra, exploiting the banded structure of the differentiation matrices. In this work, a 7-points stencil is used, which results in the optimal balance between convergence of results and computational cost. The same stencil is used for first and second order differentiation matrices, which allows for the control of the matrix structure, improving the efficiency of the sparse implementation. PSE are marched along the streamwise direction using an implicit Euler scheme. The necessary sparse matrix inversions are done using the package MUMPS [2]. Further details on the numerics can be found elsewhere [15, 13].

3.2 Results

The three-dimensional separation bubbles $\mathbf{q}_{3D}$ resulting from the saturation of the primary

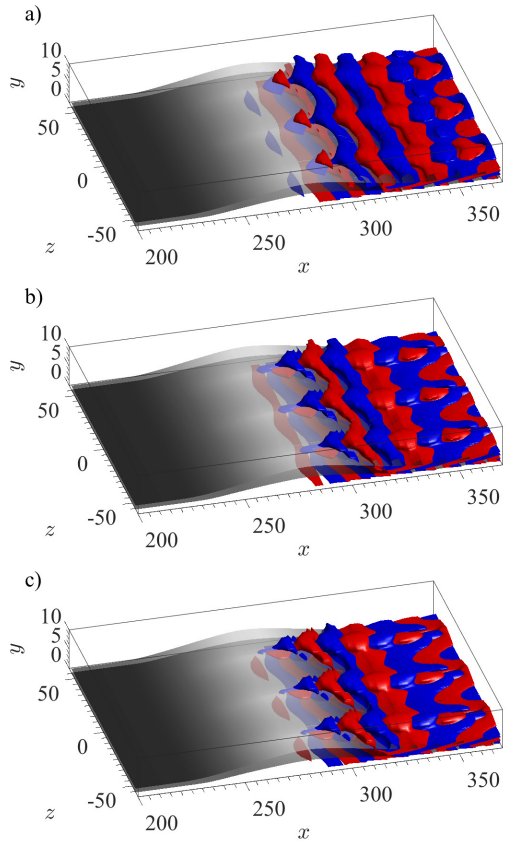

Fig. 5 Convective amplification of initially plane T-S waves. The surfaces correspond to $\omega_z' = \pm 0.1$ of the disturbance's spanwise vorticity component. The disturbance field is normalized with $\|\omega_z'\|_\infty = 1$. Grey surfaces correspond to $u_0 = 0$ and 0.5 of the 3D LSBs $\mathbf{q}_{3D}$. (a) $u_{0,rev} = 6.99\%$, (b) 7.02%, (c) 7.06%. The frequency for the maximum $N-$factor is considered for each case.

self-excited instability, and the baseline two-dimensional LSBs $\mathbf{q}_0$ are taken as the base flows $\bar{\mathbf{q}}$ in the analyses. A relatively narrow range of reversed flow magnitudes around the critical conditions for the self-excited primary instability is considered: $u_{0,rev} \approx 6.85 - 7.55\%$, $\bar{\delta}_{max} = 6.5 - 7.0$. These base flows have boundary-layer separation at $x_s \approx 220 - 222$ and reattachment at $x_r \approx 320 - 325$, which corresponds to $Re_L \approx 37,600 - 38,200$.

The arbitrary cross-section $x_0 = 100$ is chosen as inlet. The spanwise domain size is adjusted to be one wavelength of the primary instability, i.e. $L_z = \lambda_z = 2\pi/\beta_c$, and periodicity is imposed on this direction. The complex wavenumber α and shape function $\hat{\mathbf{q}}$ corresponding to the plane ($\beta = 0$) T-S wave for each ω are imposed as inlet conditions. The maximum $N-$factor computed for each separation bubble is shown in figure 4. The maximum amplification for the two-dimensional bubbles rises moderately from $N = 9.57$ ($u_{0,rev} = 6.85\%$) to $N = 9.86$ ($u_{0,rev} = 7.55\%$). Conversely, a remarkable increase in the maximum amplification follows from the three-dimensionality of the separation bubble, reaching values $N \approx 12.5$ for the base flow $\mathbf{q}_{3D}$ corresponding to $u_{0,rev} = 7.29\%$.

The spatial structure of the disturbance waves corresponding to the maximum amplitude conditions is discussed next. Three-dimensional bubbles with $u_{0,rev} = 6.99 - 7.06\%$ are shown in figure 5. Three spanwise periods are shown in the figure, to ease the visualisation of the peak and valley structures. Disturbance waves, spanwise-homogeneous at introduction and upstream of separation, are distorted by the spanwise-varying separation bubble. Disturbance amplitude peaks are aligned with the spanwise planes of higher reversed flow, while the minimum disturbance amplitudes are aligned with the spanwise planes of lesser reversed flow. In the three-dimensional steady LSBs $\mathbf{q}_{3D}$, a positive streamwise streak follows downstream of the reversed-flow peak, which distorts the relative phases of the disturbance waves along the spanwise direction. The result resembles pairs of oblique waves, that seemingly arise from the peak reversed-flow locations in the figures.

The aspect ratio between the spanwise and streamwise periodicity lengths, $\lambda_z/\lambda_x = \alpha/\beta_c$, is also shown for each case. The streamwise wavelength in the reversed flow region downstream of the maximum wall-normal extent of the bubble, the streamwise wavenumber only a slight variation with $u_{0,rev}$, and the aspect ratio $\lambda_z/\lambda_x \approx 1.93 - 2.1$. These values are in excellent agreement with experimental visualisations using particle image velocimetry on LSBs formed on a flat plate [9] and on the lee-side of an airfoil [7], in which spanwise-modulated vortical structures were found to appear in the absence of explicit forcing. The frequencies corresponding to maximum amplitudes in terms of the Strouhal number defined using the momentum thickness and free-stream velocity at separation, in order to allow for comparison with other results in the literature. The Strouhal number for which the maximum amplitudes are attained lay in the range $St_\theta = 0.0094 - 0.0104$, which agrees well with the reported experimental measurements on unforced flat-plate LSBs [17, 18, 9].

4 Conclusion

Recirculating flows, and laminar separation bubbles in particular are unstable with respect to a three-dimensional instability of centrifugal nature. This instability is self-excited, and becomes active for weaker reversed flows than required for the onset of self-excited oscillations that would lead to vortex shedding. On account of this instability, LSBs develop a spanwise-periodic modulation in terms of size and recirculation intensity.

Wind-tunnel experiments show that LSBs are dominated by the convective amplification of disturbance waves that are originated well upstream of the separation, and that exhibit large growths in the separated shear layer due to the inflectional instability. This paper shows that the three-dimensionality of the separated shear layer impacts on the amplification of disturbance waves originated upstream. The total amplification is drastically increased, with the maximum $N-$factor shifting from $N = 9.747$ to $N = 12.495$

for the same conditions. The LSB's streamwise vorticity distorts the initially two-dimensional T-S waves periodically along the spanwise direction resulting into an arrangement that resembles pairs of oblique waves. The aspect ratio of the wavy disturbances in the aft portion of the separation bubble, $\lambda_z/\lambda_x \approx 1.94 - 2.01$, is similar to reported experiments which considered LSBs without explicit forcing [7, 9]. The organized oblique wave pattern together with the strong spatial amplification suggests an oblique transition scenario akin to that proposed by [10].

Acknowledgments

The authors acknowledge funding from CNPq (grants 405144/2016-4, 305512/2016-1, 423846/2016-7), FAPESP (grants 2014/24782-0, 2017/01586-0) and FAPERJ (grants 223669, 233386)

References

[1] M. Alam and N. D. Sandham. Direct numerical simulation of 'short' laminar separation bubbles with turbulent reattachment. *J. Fluid Mech.*, 410:1–28, 2000.

[2] Patrick R. Amestoy, Iain S. Duff, Jean-Yves L'Excellent, and Jacko Koster. A fully asynchronous multifrontal solver using distributed dynamic scheduling. *SIAM J. Matrix Anal. Appl.*, 23(1):15–41, 2001.

[3] M. Broadhurst and S. Sherwin. The parabolised stability equations for 3d-flows: implementation and numerical stability. *Applied Numerical Mathematics*, 58(7):1017 – 1029, 2008.

[4] S.S. Diwan and O.N. Ramesh. On the origin of the inflectional instability of a laminar separation bubble. *J. Fluid Mech.*, 629:263–298, 2009.

[5] A.V. Dovgal, V.V. Kozlov, and A. Michalke. Laminar boundary layer separation: instability and associated phenomena. *Prog. Aero. Sci.*, 3:61–94, 1994.

[6] T. Herbert. Parabolized stability equations. *Ann. Rev. of Fluid Mechanics*, 29:245–283, 1997.

[7] J. W. Kurelek, A. R. Lambert, and S. Yarusevych. Coherent structures in the transition process of a laminar separation bubble. *AIAA J.*, 54(8):2295–2309, 2016.

[8] O. Marxen, M. Lang, and U. Rist. Vortex formation and vortex breakup in laminar separation bubbles. *J. Fluid Mech.*, 728:58–90, 2013.

[9] T. Michelis, S. Yarusevych, and M. Kotsonis. On the origin of spanwise vortex deformations in laminar separation bubbles. *J. Fluid Mech.*, 841:81–108, 2018.

[10] U. Rist and U. Maucher. Direct numerical simulation of 2–d and 3–d instability waves in a laminar separation bubble. In B. Cantwell, editor, *AGARD-CP-551 Application of Direct and Large Eddy Simulation to Transition and Turbulence*, pages 34–1 – 34–7, 1994.

[11] U. Rist and U. Maucher. Investigations of time-growing instabilities in laminar separation bubbles. *Eur. J. Mech. B/Fluids*, 21:495–509, 2002.

[12] D. Rodríguez and E. M. Gennaro. Three-dimensional flow stability analysis based on the matrix-forming approach made affordable. In J. S. Hesthaven, editor, *International Conference on Spectral and High-Order Methods 2016*, Lecture Notes in Computational Science and Engineering. Springer, 2017.

[13] D. Rodríguez and E. M. Gennaro. Enhancement of disturbance wave amplification due to the intrinsic three-dimensionalisation of laminar separation bubbles. *The Aeronautical Journal*, under review.

[14] D. Rodríguez, E. M. Gennaro, and M. P. Juniper. The two classes of primary modal instability in laminar separation bubbles. *J. Fluid Mech.*, 734:R4, 2013.

[15] D. Rodríguez, M. R. Jotkar, and E. M. Gennaro. Wavepacket models for subsonic twin jets using 3d parabolized stability equations. *Comptes Rendus Mec.*, in print, 2018.

[16] D. Rodríguez and V. Theofilis. Structural changes of laminar separation bubbles induced by global linear instability. *J. Fluid Mech.*, 655:280–305, 2010.

[17] J. Serna and B. J. Lázaro. The final stages of transition and the reattachment region in transitional separation bubbles. *Exp. Fluids*, 55:1695, 2014.

[18] J. Serna and B. J. Lázaro. On the bursting condition for transitional separation bubbles. *Aerosp.*

Sci. Technol., 44:43–50, 2015.

[19] P.R. Spalart and M. Kh. Strelets. Mechanisms of transition and heat transfer in a separation bubble. *J. Fluid Mech.*, 403:329–349, 2000.

[20] V. Theofilis, S. Hein, and U. Dallmann. On the origins of unsteadiness and three-dimensionality in a laminar separation bubble. *Phil. Trans. Roy. Soc. London (A)*, 358:3229–3246, 2000.

[21] J. H. Watmuff. Evolution of a wave packet into vortex loops in a laminar separation bubble. *J. Fluid Mech.*, 397:119–169, 1999.

Contact Author Email Address

danielrodriguez@id.uff.br

Copyright Statement